Journal of Environmental Chemical Engineering 5 (2017) 3384–3394

Contents lists available at ScienceDirect

Journal of Environmental Chemical Engineering

journal homepage: www.elsevier.com/locate/jece

Acid Blue 113 removal from aqueous solution using novel biosorbent based on NaOH treated and surfactant modified fallen leaves of *Prunus Dulcis*

Suyog N. Jain, Parag R. Gogate*

Chemical Engineering Department, Institute of Chemical Technology, Nathalal Parekh Marg, Matunga, Mumbai 400019, India

ARTICLE INFO

Keywords:
Acid blue 113
Adsorption
Azo dyes
Thermodynamics
Desorption

ABSTRACT

In the present work, the fallen leaves of *Prunus Dulcis* (almond) have been used for obtaining biosorbent with activation based on NaOH and surfactant treatment. Characterization of biosorbent was performed using Fourier transform infrared spectroscopy, scanning electron microscopy, elemental analysis and Brunauer–Emmett–Teller analysis techniques. The obtained biosorbent was subsequently applied for removal of azo dye, Acid Blue 113, from aqueous solution. The effects of biosorbent dose, contact time, initial dye concentration, salt concentration and temperature on the extent of adsorption of AB 113 were investigated in batch mode. The optimum conditions obtained for maximum dye removal were biosorbent dose of 10 g L^{-1} for NaOH treated biosorbent and 3 g L^{-1} for surfactant modified biosorbent, contact time of 2.5 h and temperature of 293 K. Better results were obtained for surfactant modified biosorbent (almost 100% removal) as compared to the NaOH activated biosorbent. The adsorption kinetics data were found to be well described by pseudo-second order equation whereas Langmuir and Temkin isotherm models were observed to be best fitted to the obtained equilibrium data. The adsorption was found to be exothermic and spontaneous in nature. Maximum biosorption capacity obtained under optimized conditions were 10.87, 25.51 and 97.09 mg g^{-1} for conventionally obtained biosorbent, NaOH treated biosorbent and surfactant modified biosorbent respectively. Regeneration studies and subsequent application demonstrated potential of the biosorbent for dye removal in more than one cycle. The present study conclusively established the potential of surfactant modified biosorbent for effective removal of Acid Blue 113 dye with significantly higher biosorption capacity of 97.09 mg g^{-1} in comparison with other commonly used adsorbents.

1. Introduction

One of the largest contributors to the environmental issues arising from industrial wastewater is the textile industry as large quantity of the water is consumed, which in turn also generates large amount of effluent containing hazardous and biorefractory pollutants. Dyeing process is one of the major pollution sources of textile wastewater [1]. More than 10,000 synthetic dyes are available commercially and annual worldwide production of dyes is over 7×10^5 tones [2]. During dyeing process, 10–15% of the dye is released into the process effluent which can also find its ways into water bodies [3]. One of the most widely used class of dyes is azo dyes and account for over 60% of the total dye consumption [4]. Azo dyes are widely used in a variety of industries like paper, textile, food, leather and cosmetic industries and contribute to significant pollution [5]. Chemical structure of azo dyes contains aromatic and azo group, which contribute to their toxic and non-biodegradable nature [6]. Toxic nature of azo dyes is also due to presence of amines [7]. Azo dyes can cause skin irritation, allergy and mutation. These dyes can reduce light transmission and affect photosynthesis process, which can alter the ecological balance [8]. Hence it is imperative to develop effective approaches to remove azo dyes from wastewater and protect the environment.

Wide range of methods have been applied by researchers for the treatment of azo dyes containing wastewater such as ozonation [9], cloud point extraction [10], photocatalytic degradation [11], electrochemical degradation [12] and nanofiltration [13]. Adsorption is considered to be efficient technique for dyes removal from aqueous solution due to its simplicity, ease of operation and ability to give high quality treated effluent. The most efficient and widely used adsorbent for dyes removal from aqueous solution is activated carbon [14]. The worldwide consumption of activated carbon is continuously increasing due to its application for control of pollution [15]. But it suffers from limitation of high cost, as in many countries, activated carbon is produced from nonrenewable and costly materials such as coal and timber [16]. This limitation has motivated scientific community to search for low cost and easily available sustainable adsorbents as a replacement to

* Corresponding author.
E-mail addresses: pr.gogate@ictmumbai.edu.in, paraggogate@yahoo.co.in (P.R. Gogate).

http://dx.doi.org/10.1016/j.jece.2017.06.047
Received 18 March 2017; Received in revised form 20 May 2017; Accepted 25 June 2017
Available online 27 June 2017
2213-3437/

activated carbon [17]. One of the approaches to obtain low cost adsorbent is based on utilization of agricultural solid waste. Carboxyl, hydroxyl and amine groups present on the surfaces of waste materials make them an attractive proposition for pollutant removal by adsorption. Use of agricultural waste as an adsorbent also offer the advantages of reduction in solid waste and low cost [18].

Various low cost alternatives in their raw form (without any activation) have been applied by researchers such as beach bivalve shells [19], Phoenix dactylifera seeds [20], Argemone mexicana seeds [21], green leaves of Paulownia tomentosa Steud. [22], marble dust [23] and sugar beet pulp [24] for the specific application of dyes removal. Researchers have also tried different activation methods to enhance the adsorption capacity of the naturally available low cost adsorbents [25] such as NaOH treatment applied to ficus racemosa [26], formaldehyde treatment applied to sawdust [27], H_2SO_4 treatment applied to montmorillonite [28], surfactant treatment applied to wheat straw [29] and $CaCl_2$ treatment applied to bentonite [30]. A literature survey revealed that researchers have not used fallen tree leaves of *Prunus Dulcis* (almond), for biosorbent synthesis and subsequent application for the removal of azo dye, Acid blue (AB) 113 has also not been investigated. In the present study, fallen leaves of *Prunus Dulcis* (FLPD), which is an abundantly available sustainable biomass especially in India, has been selected as the feed stock for synthesis of biosorbent and activation treatment based on NaOH and cationic surfactant has been given with an objective of obtaining efficient biosorbent which can give maximum sorption capacity. NaOH and surfactant activation can help to increase surface area based on developing significant pores in the biosorbent. The testing of the adsorption capacity has been performed based on the application of removal of AB 113, an azo dye, from aqueous solution. AB 113 is used for dyeing wool, fabric, nylon and leather [31]. AB 113 is typically an anionic dye and hence biosorbent has been modified using cationic surfactant so that dye will be selectively adsorbed based on an electrostatic attraction. Literature survey revealed that a cationic surfactant, cetyl trimetyl ammonium bromide (CTAB) gave better results for different anionic compounds and azo dye removal [32,33]. Considering this analysis, in the present study, CTAB was used for the modification of the biosorbent.

2. Materials and methods

2.1. Biosorbent synthesis and characterization

FLPD were collected from Nashik, India. Leaves were washed thoroughly with distilled water and dried in sunlight to evaporate the moisture. Leaves were then crushed into powder and sieved to get particle size in the range of 53–106 μm. The PD leaves powder thus obtained was impregnated with 1% by weight NaOH solution in the ratio of 1:5 and heated in oven at 323 K for 4 h to remove lignin based color of the powder. The PD powder was then filtered and washed with distilled water to remove free NaOH and thermally activated in oven at 353 K for 24 h. The NaOH treated PD biosorbent (NTPD) was placed in airtight container. Surfactant modified biosorbent was also prepared using the following procedure: 200 mL of 1% CTAB [$C_{19}H_{42}BrN$], is prepared. In this surfactant solution, 5 g of NTPD was added. The mixture was shaken in orbital shaking incubator (Bio-Technics, India) at 100 rpm for 12 h at room temperature. Solution was then filtered and washed with distilled water to remove superficially retained CTAB. Finally, surfactant modified PD biosorbent (SMPD) was dried at 333 K overnight and stored in an airtight container for further study.

Scanning electron microscope (SEM, JEOL-6380, USA) was used to determine surface characteristics and morphology of both NTPD and SMPD biosorbent. Fourier transform infrared spectroscopy (FTIR, Perkin Elmer Spectrum BX, USA) was used to determine the functional groups present on the biosorbents which can be useful for removal of AB 113 from wastewater. FTIR spectra of biosorbents were recorded at room temperature over a range of 400–4000 cm^{-1} using KBr pellet. The weight percentage of carbon, hydrogen, nitrogen and sulfur in NTPD and SMPD were determined using CHNS elemental analyzer (Thermo Finnigan, Italy). Surface area, pore volume and pore diameter of the FLPD, NTPD and SMPD biosorbents were determined using the Brunauer-Emmett-Teller (PMI BET Sorptometer- 201AEL-2OSEL, USA) analyzer.

2.2. Dye used in the work for adsorption studies

AB 113 dye [C.I. = 26360, molecular formula = $C_{32}H_{21}N_5Na_2O_6S_2$, molecular weight = 681.65 g mol^{-1}], selected in the present study was obtained from Sigma-Aldrich, Mumbai as analytical grade dye. AB 113 dye was in the form of dark blue powder. Stock solution of initial dye concentration as 1000 mg L^{-1} was prepared by dissolving 1 g of dye in 1 L of distilled water. Stock solution was then diluted with distilled water to prepare working solutions of desired dye concentrations.

2.3. Analysis of dye

The quantification of AB 113 in the residual solutions was performed using UV–vis Spectrophotometer (UV 1800, Shimadzu, Japan) at λ_{max} of 566 nm. Calibration curve of AB 113 dye was established over the dye concentration range of 1 to 100 mg L^{-1}. In this range, linearity was observed between absorbance and concentration with correlation coefficient (R^2) of 0.9991. Limit of detection (LOD) and limit of quantification (LOQ) are important parameters in validation, which are determined using standard deviation and slope of the calibration curve. LOD and LOQ were 0.068 and 0.226 mg L^{-1} respectively established for the calibration curve of AB 113 dye.

2.4. Experimental methodology

Batch adsorption experiments were conducted to establish the variation in the efficacy of adsorption of AB 113 dye with varying biosorbent dose, contact time, initial dye concentration, salt concentration and temperature. AB 113 dye is an acidic dye hence its removal can be maximum at lower pH values but color of AB 113 dye solution was found to change in strongly acidic medium whereas color change was not found to be significant in slightly neutral or alkaline medium. Dye was found to be stable at natural pH of 6.5 and hence all experiments were performed at natural pH of dye solution, which can also give advantage in actual commercial processing as any pH adjustments will not be required. Batch experiments were performed by taking 50 mL of AB 113 dye solution of desired concentration in 100 mL conical flasks. A desired quantity of biosorbent was added into the dye solution and solution was subjected to agitation in orbital shaking incubator for desired contact time at 150 rpm and at the selected temperature. Samples were withdrawn from orbital shaking incubator at desired time intervals and subjected to centrifugation in a research centrifuge (Remi scientific works, Mumbai) at speed of 8000 rpm to remove suspended particles. Supernatant samples were then analyzed using UV–vis Spectrophotometer to determine concentration of dye remaining in the solutions. The effect of biosorbent dose was studied over the range of 1–20 g L^{-1} for NTPD and 0.2–6 g L^{-1} for SMPD at constant temperature of 303 K. The effluent from dye processing unit generally contains 150 to 330 mg L^{-1} of unused dye [34]. Accordingly in the present study, effluents were prepared synthetically starting from a minimum concentration of AB 113 dye as 50 to maximum of 450 mg L^{-1}. Effect of contact time on the dye removal was studied at different dye concentrations in the range of 50–200 mg L^{-1}, at constant temperature of 303 K, and biosorbent dose of 3 g L^{-1} for SMPD. Effect of salt concentration over the range of 0.01 to 0.1 mol L^{-1} was also studied using 100 mg L^{-1} of initial dye concentration at constant temperature of 303 K, and biosorbent dose of 3 g L^{-1} for SMPD. The equilibrium study was also performed at varying temperatures of 293, 303, 313 and 323 K for an initial AB dye concentration in the range of 50–400 mg L^{-1} (nine

different initial concentrations for each temperature) for FLPD and NTPD and 50–450 mg L^{-1} (ten different initial concentrations for each temperature) for SMPD. Regeneration studies were performed for three cycles by conducting adsorption experiments of 100 mg L^{-1} of AB 113 dye on SMPD with desorption of dye being carried out using ethanol, as an eluent, after every cycle of use. All the batch experiments were performed in triplicates and mean values were used to evaluate the kinetic, isotherm and thermodynamic parameters.

Amount of AB 113 dye adsorbed on the biosorbent was obtained using the following equation:

$$q_t = \frac{(C_i - C_t)V}{M} \tag{1}$$

Where q_t is biosorption capacity (mg g^{-1}), expressed as mg of dye adsorbed per g of biosorbent at any time t, C_i and C_t are the initial dye concentration and dye concentration (mg L^{-1}) at any time t, respectively, V is volume of dye solution (L) and M is quantity of the biosorbent used (g).

2.5. Adsorption kinetics

In the present study, pseudo first-order, pseudo second-order, intra-particle diffusion and Bangham pore diffusion model have been used to check the fitting of the adsorption kinetic models with the obtained data.

2.5.1. Pseudo first-order model

Pseudo first-order model equation is expressed as follows [35]:

$$\frac{dq_t}{dt} = k_1(q_e - q_t) \tag{2}$$

Where, k_1 is pseudo first-order rate constant (min^{-1}) and q_e is biosorption capacity at equilibrium (mg g^{-1}).

After integrating and applying the boundary condition, the obtained equation is:

$$\ln(q_e - q_t) = -k_1 t + \ln q_e \tag{3}$$

k_1 value was calculated from the slope ($-k_1$) and $q_{e,cal}$ value was calculated from the intercept ($ln\ q_e$) of the plot of $ln\ (q_e\text{-}q_t)$ versus t.

2.5.2. Pseudo second-order model

Pseudo second-order model equation is expressed as follows [36]:

$$\frac{dq_t}{dt} = k_2(q_e - q_t)^2 \tag{4}$$

Where k_2 is pseudo second-order rate constant (g mg $^{-1}$ min^{-1}).

After integrating and applying the boundary condition, the obtained equation is:

$$\frac{t}{q_t} = \frac{t}{q_e} + \frac{1}{k_2 q_e^2} \tag{5}$$

$q_{e,cal}$ value was calculated from the slope ($1/q_e$) and k_2 value was calculated from the intercept ($1/k_2 q_e^2$) of the plot of t/q_t versus t.

2.5.3. Intra-particle diffusion model

One of the important factors in the successful scale up of adsorption is determination of rate controlling step. Therefore, the obtained kinetic data were analyzed by Weber-Morris intra-particle diffusion model, expressed as follows [37]

$$q_t = k_{id} t^{1/2} + C \tag{6}$$

Where k_{id} which is the rate constant for intra-particle diffusion (mg g^{-1} $min^{-1/2}$) is estimated as the slope and intercept, C represents boundary layer thickness (mg g^{-1}).

2.5.4. Bangham pore diffusion model

Bangham model is mathematically expressed as follows [38]

$$log\left(log\left(\frac{C_i}{C_i - q_t m}\right)\right) = \alpha log t + log\left(\frac{k_0 m}{2.303V}\right) \tag{7}$$

Where m is biosorbent dose (g L^{-1}), V is volume of dye solution (mL), α and k_o are model parameters. The parameters, α and k_o are obtained from slope and intercept of the logarithmic plot of above equation.

2.6. Biosorption equilibrium adsorption isotherm study

In the present study, Freundlich, Langmuir and Temkin adsorption models are used for isotherm analysis.

Linearized form of Freundlich isotherm model [39] is expressed as follows:

$$lnq_e = \frac{1}{n}\ lnc_e + lnK_F \tag{8}$$

Where K_F is Freundlich isotherm constant (mg g^{-1})/(mg L^{-1}) $^{1/n}$ and $1/n$ is heterogeneous factor (dimensionless).

Linearized form of Langmuir isotherm model [40] is expressed as follows:

$$\frac{c_e}{q_e} = \left(\frac{1}{q_m}\right)\ C_e + \frac{1}{q_m K_L} \tag{9}$$

Where q_m represents maximum biosorption capacity (mg g^{-1}) and K_L is Langmuir biosorption constant (L mg^{-1}) indicating affinity of AB 113 dye towards the biosorbent.

Linearized form of Temkin isotherm model [41] is expressed as follows:

$$q_e = B \ln c_e + B \ln K_T \tag{10}$$

Where B (mg g^{-1}) and K_T (L mg^{-1}) are Temkin isotherm constants. K_T indicates the biosorption affinity.

Average relative error (ARE) function values have been calculated to determine the most suitable isotherm model to fit the experimental data. The ARE error function [42] is given as follows:

$$ARE = \frac{100}{n}\sum_{i=1}^{n}\left|\frac{(q_{e,\exp} - q_{e,calc})}{q_{e,\exp}}\right|_i \tag{11}$$

Where n is number of data points, $q_{e,exp}$ is the experimental value of q_e and $q_{e,cal}$ is the calculated value of q_e using the fitted isotherm model.

2.7. Adsorption thermodynamics

The thermodynamic parameters such as free energy change, ΔG^0 (kJ mol^{-1}), enthalpy change, ΔH^0 (kJ mol^{-1}) and entropy change, ΔS^0 (kJ mol^{-1} K^{-1}) have a significant role in determining the feasibility, spontaneity and nature of the biosorption process. These parameters can be estimated by Van't Hoff equation, given as follows:

$$\Delta G^0 = -RT \ln K \tag{12}$$

Where R is universal gas constant (8.314 J mol^{-1} K^{-1}), T is absolute temperature (K) and K is equilibrium constant.

ΔG^0, ΔH^0, ΔS^0 and T are also related by the following equation:

$$\Delta G^0 = \Delta H^0 - T\Delta S^0 \tag{13}$$

By combining above two equations, we obtain the following new equation used for obtaining the required thermodynamic parameters.

$$lnK = -\frac{\Delta H^0}{R}\frac{1}{T} + \frac{\Delta S^0}{R} \tag{14}$$

2.8. Activation energy of biosorption

The activation energy for biosorption of AB 113 on SMPD was calculated from pseudo second order rate constant values using the Arrhenius equation given as follows [43]:

$$lnk_2 = -\frac{E_a}{RT} + lnA \quad (15)$$

Where k_2 is pseudo second-order rate constant (g mg^{-1} min^{-1}), E_a is activation energy (kJ mol^{-1}) and A is Arrhenius constant (g mg^{-1} min^{-1}). E_a has been found from the slope of plot of $ln\ k_2$ versus $1/T$.

2.9. Reusability study

Desorption efficiency has also been calculated using following equation [44]:

$$\text{Desorption efficiency}(\%) = \frac{C_{des}}{C_{ads}} \times 100 \quad (16)$$

Where C_{des} is concentration of dye adsorbed on the adsorbent in the reuse and C_{ads} is concentration of dye (mg L^{-1}) adsorbed on the adsorbent in the original cycle.

3. Results and discussion

3.1. Characterization of biosorbent

Fig. 1 depicts scanning electron microscopy images of the different biosorbents obtained in the present work. The microscopic image in Fig. 1a shows that surface of NTPD is irregular and characterized by the presence of microscopic pores of different sizes. SEM images depicted in Fig. 1a and b establish that the surface of both the biosorbents (NTPD and SMPD) is fibrous and rough which can be considered as excellent characteristic with high possibility for AB 113 dye to be trapped and adsorbed on the surface. It can be also seen that the surface morphology of SMPD (Fig. 1b) is different than NTPD which is due to coverage of CTAB molecules on the surface. Fig. 1c shows the images of SMPD after use in adsorption confirming the coverage by dye molecules. The FTIR analysis of NTPD biosorbent, SMPD biosorbent before and after adsorption of AB 113 dye have been shown in Fig. 2a–c respectively. The peaks at 2924.09 and 2854.65 cm^{-1} in Fig. 2b are attributed to asymmetric and symmetric C—H stretching vibrations of methylene group [20]. The new peak of methylene group at 2854.65 cm^{-1} in Fig. 2b confirms the linkage of surfactant to the biosorbent. The peak at 2924.09 cm^{-1} is sharpened in Fig. 2b as compared to Fig. 2a thus indicating increase in number of carbon atoms after the surfactant treatment [32]. The peak at 1435.04 cm^{-1} in Fig. 2a can be attributed to stretching vibration of CH_2 and CH_3 [45]. It gets shifted to 1458.18 cm^{-1} (Fig. 2b) after surfactant treatment indicating linkage of surfactant aliphatic molecules on the biosorbent. The broad band at 3346.57 cm^{-1} in NTPD (Fig. 2a) attributed to presence of —NH and/or —OH stretching vibrations of amine and/or hydroxyl group appears to be shifted to lower value 3340.71 cm^{-1} (Fig. 2b) after surfactant treatment. The same peak gets shifted to 3348.42 cm^{-1} after dye adsorption (Fig. 2c) indicating the interaction between SMPD biosorbent and AB 113 dye [46]. The peak at 1728.22 cm^{-1} can be attributed to presence of carboxyl group on the biosorbent which gets shifted to 1712.79 cm^{-1} for the biosorbent after adsorption of dye. The peak at 1319.31 cm^{-1} can be attributed to C—N stretching which gets shifted to 1327.03 cm^{-1} again attributed to the adsorption of dye on the biosorbent surface [47]. The strong peak at 1612.49 cm^{-1} can be attributed to C═O stretching of carboxylic group present on the biosorbent surface [48]. The peaks at 1558.48 and 1180.44 cm^{-1} in Fig. 2c can be attributed to azo group, —N═N— and sulfate group, S═O of AB 113 dye, respectively confirming the adsorption of dye on biosorbent [49].

Elemental analysis was also performed to compare the composition of NTPD and SMPD. The weight percentages of elements were observed to be 40.391% C, 4.435% H, and 0.338% N for NTPD and 47.845% C, 6.155% H, and 1.136% N for SMPD. An increase in percentages of C, H and N in SMPD were observed as a result of surfactant treatment. The obtained results of FT-IR and elemental analysis confirmed the effective linkage of CTAB on the surface of NTPD.

The obtained data for the BET surface area, total pore volume and average pore diameter have been depicted in Table 1. BET specific surface area was seen to significantly increase from 67.02 for FLPD to 426.35 m^2 g^{-1} for NTPD by NaOH treatment. It decreased from 426.35 to 243.64 m^2 g^{-1} during the treatment of NTPD with surfactant which can be attributed to blocking of NTPD pores by alkyl chains of surfactant. There is slight increase in average pore diameter due to surfactant treatment of NTPD which is presumably due to elimination of microstructure of NTPD. It is important to note that the surface area is not the only factor driving the adsorption as discussed in the subsequent section of adsorption mechanism.

3.2. Adsorption mechanism

In the present study, fallen leaves, a natural substrate has been activated using NaOH and surfactant treatment. NaOH treatment removes colored lignin from the biosorbent which can interfere with the deposition of the dye. The treatment also develops significant pores in the biosorbent and hence offers increased surface area and pore volume for the biosorbent [50] as can be easily seen from the data represented in Table 1. In other words, NaOH treatment made the surface porous which is favorable condition for dye adsorption and thus increased biosorption capacity of the fallen leaves. Biosorption capacity was further enhanced by surfactant treatment. Cationic surfactant treatment developed positive charge on the biosorbent. The adsorption of CTAB on the surface of the biosorbent involves interaction of CTAB molecules

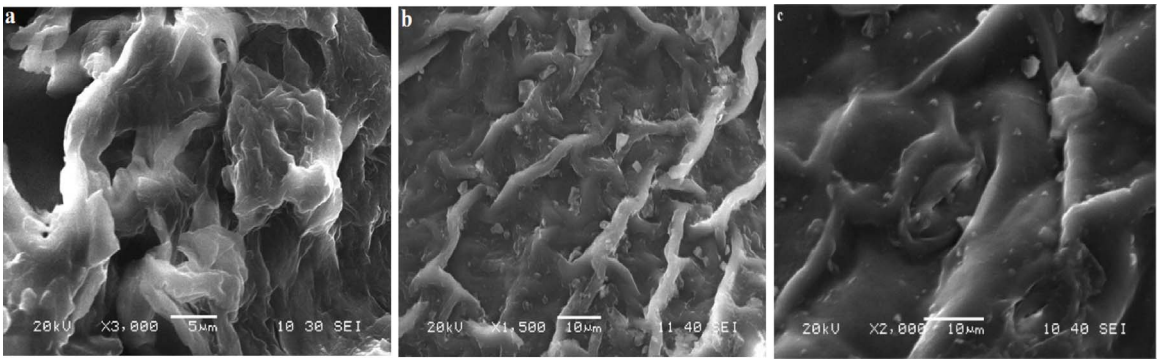

Fig. 1. Scanning electron microscopy images of a) NTPD b) SMPD before adsorption c) SMPD after adsorption.

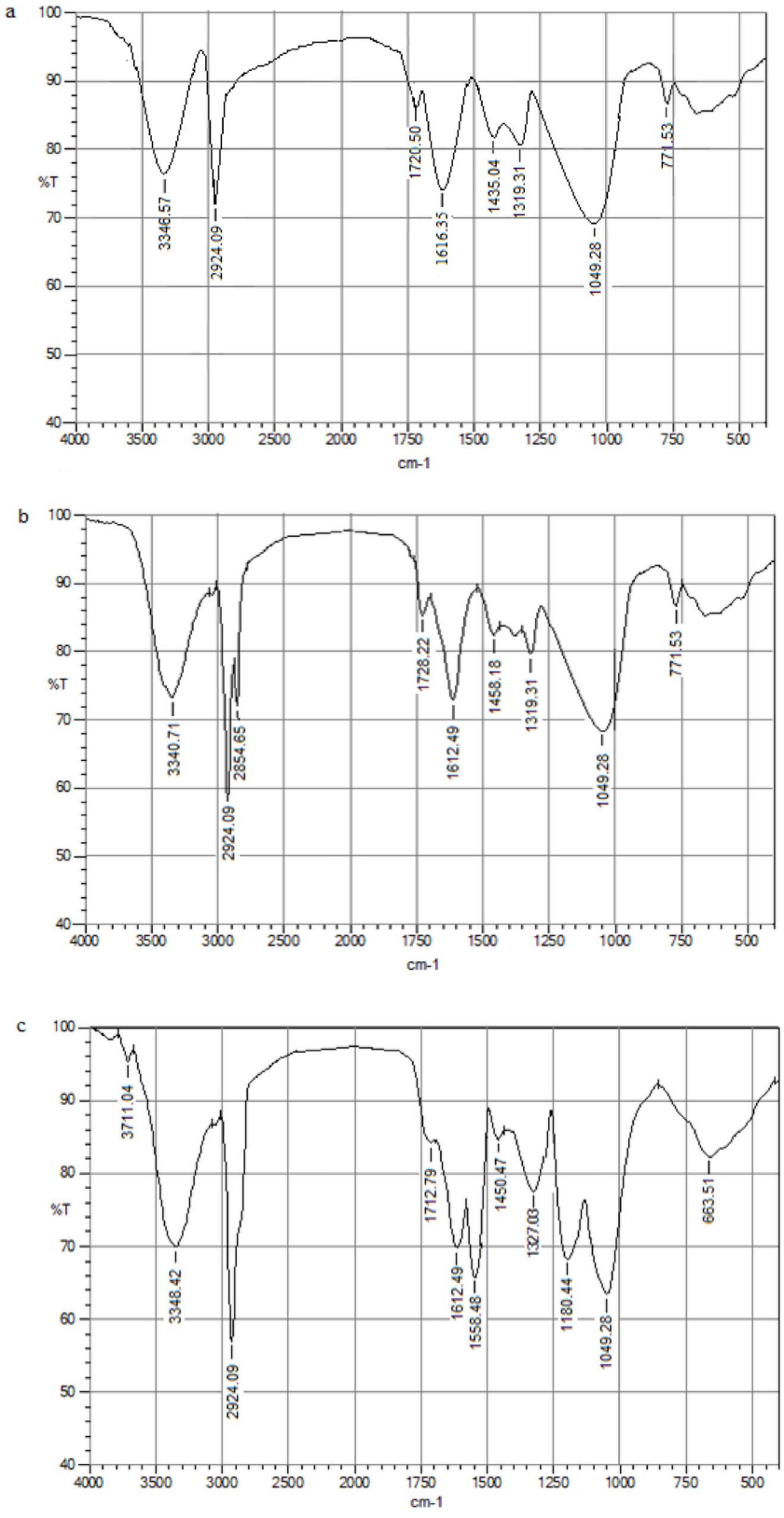

Fig. 2. FT-IR spectra of a) NTPD b) SMPD before adsorption c) SMPD after adsorption.

with NTPD through their alkyl groups; hence positive head of CTAB points toward bulk of the dye solution used in the current work. Thus the electrostatic attraction between the negatively charged SO_3 group of AB 113 dye molecules and organic cationic groups on SMPD is expected to be the main phenomenon for the intensified adsorption of AB 113 dye. Van der Waals force of interaction between the phenyl ring of AB 113 and CH_2 group of SMPD through hydrogen bonds will also be an additional driving force for the efficient adsorption of dye on SMPD [51].

Table 1
BET surface area, total pore volume and average pore diameter for FLPD, NTPD and SMPD.

Adsorbent sample	Surface area ($m^2\ g^{-1}$)	Total pore volume ($cm^3\ g^{-1}$)	Average pore diameter (nm)
FLPD	67.02	0.0622	3.713
NTPD	426.35	0.2818	2.644
SMPD	243.64	0.1617	2.654

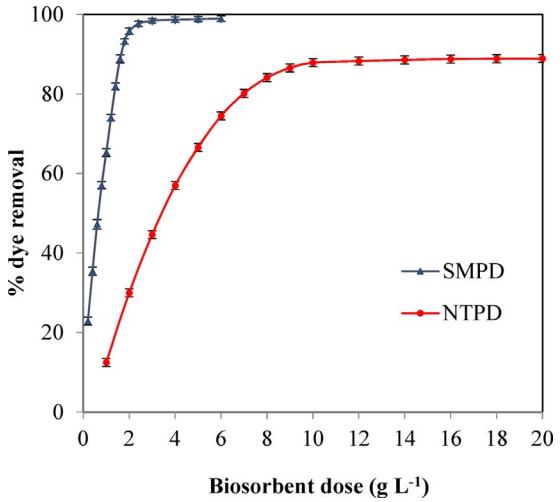

Fig. 3. Effect of biosorbent dose on the removal of AB 113 using NTPD and SMPD (T = 303 K, t = 2.5 h, C_i = 100 mg L^{-1}).

3.3. Effect of biosorbent loading (m)

The effect of biosorbent loading on the removal of AB 113 was studied by varying the biosorbent loading from 1 to 20 g L^{-1} for NTPD and from 0.2 to 6 g L^{-1} for SMPD (Fig. 3). Dye removal was found to be increased from 12.48 ± 1.16% % at 1 g L^{-1} to 87.84 ± 0.69% at 10 g L^{-1} for NTPD and from 22.86 ± 0.98% at 0.2 g L^{-1} to 98.41 ± 0.53% at 3 g L^{-1} loading for SMPD. Increase in dye removal percentage with an increase in biosorbent dose could be attributed to increase in the surface area of biosorbent, augmenting more number of sites being available for adsorption as well as enhanced interactions between the functional groups on the surface [52]. The dye removal slightly increased from 87.84 ± 0.69% at 10 g L^{-1} to 88.87 ± 0.64% at 20 g L^{-1} for NTPD. Similarly for SMPD, dye removal also slightly increased from 98.41 ± 0.53% at 3 g L^{-1} to 98.94 ± 0.71% at 6 g L^{-1}. It has been established that above the biosorbent dose of 10 g L^{-1} for NTPD and 3 g L^{-1} of SMPD, no significant increase in dye removal is observed, which can be attributed to binding of almost all molecules of dye on the biosorbent surface, indicating adsorption equilibrium between molecules of dye on the biosorbent surface and those present in the residual solution. Similar trend has also been reported for removal of Rhodamine B using the activated lignocellulosic waste [53]. The biosorption capacity (q_t) of NTPD and SMPD decreased with an increase in biosorbent dose beyond the optimum, which can be attributed to excess presence of active adsorption sites at high biosorbent dose. In other words, available dye molecules were not sufficient to occupy all the actives sites of biosorbent. Similar trend has also been reported for removal of congo red dye using graphene oxide/chitosan fibers [54]. The optimum biosorbent dose of 10 g L^{-1} for NTPD and 3 g L^{-1} for SMPD was used for further investigation. The results have also shown that SMPD is more efficient biosorbent for AB 113 dye removal than NTPD. Maximum dye removal at lower biosorbent dose has been observed for SMPD as compared to the NTPD, which can be attributed to the electrostatic attraction between anionic AB 113 dye molecules and cationic surfactant molecules as well as the enhanced Van der Waals force of interaction between surfactant and molecules of dye [33].

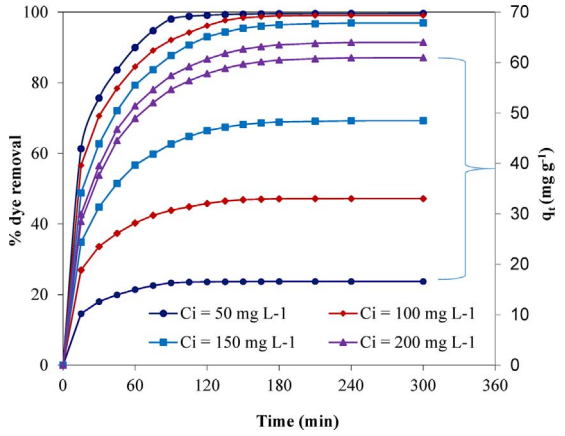

Fig. 4. Effect of contact time and initial dye concentration on dye removal and biosorption capacity of SMPD (T = 303 K, t = 5 h, C_i = 50–200 mg L^{-1}, m = 3 g L^{-1},the top four curves refer to dye removal whereas the bottom four curves highlighted by curly bracket refer to q_t).

3.4. Effect of contact time (t)

Fig. 4 depicts the effect of contact time on AB 113 dye removal by SMPD at four different initial dye concentrations of 50, 100, 150 and 200 mg L^{-1}. Dye removal was found to be almost 99% for 50 mg L^{-1} of dye concentration in 2 h and remained almost constant thereafter. But for higher dye concentrations studied in the present work, dye removal was found to increase till 2.5 h of treatment. Overall, rapid dye adsorption was found to be achieved in initial period of 30 to 60 min and thereafter, slow rate of adsorption is observed and adsorption equilibrium is reached in about 2.5 h. Adsorption was performed till 5 h of contact time and it was observed that an increase in AB 113 dye removal was less than 1% for all the concentrations as compared to contact time of 2.5 h. Based on the results, equilibrium time has been fixed at 2.5 h and all the subsequent experiments were performed for contact time of 2.5 h. During the initial periods of treatment, adsorption rate is higher as abundant quantum of empty sites is available for adsorption of dye. Afterwards, adsorption rate decreases as less number of vacant sites are available for adsorption which are difficult to be occupied as repulsive forces exist between molecules of solute on the biosorbent surface and bulk phases. Similar trend has been reported for brilliant green dye removal using NaOH treated saw dust [55].

3.5. Effect of initial dye concentration (Ci)

The initial dye concentration is an important driving force to overcome mass transfer resistance between aqueous dye solution and adsorbent surface. Fig. 4 also shows the obtained results for the effect of C_i (range 50–200 mg L^{-1}) on the extent of dye removal using SMPD. The value of q_t was found to increase from 16.61 ± 0.87 to 60.97 ± 0.73 mg g^{-1} with an increase in initial dye concentration from 50 to 200 mg L^{-1}, respectively. The observed results have been attributed to high driving force available for mass transfer at high dye concentrations, leading to transfer of dye molecules from dye solution to the biosorbent surface. Similar trend has been also reported for removal of Congo red dye using PANi/Bi_2WO_6 nanocomposites [56].

3.6. Effect of salt concentration

Dye effluent from textile industry contains high concentration of

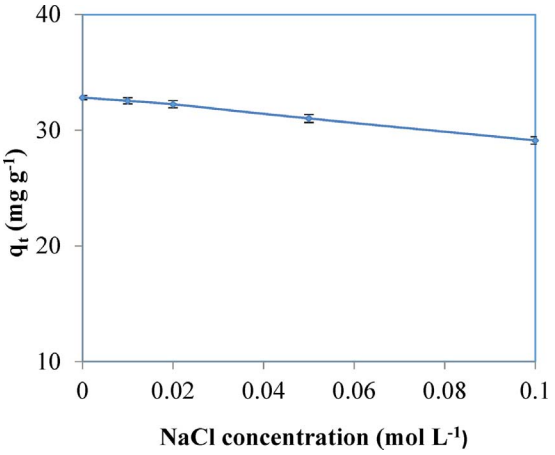

Fig. 5. Effect of salt concentration on biosorption capacity of SMPD (T = 303 K, t = 2.5 h, C_i = 100 mg L^{-1}, m = 3 g L^{-1}).

salt, which may affect adsorption of dye. In order to investigate the influence of salt concentration on biosorption capacity, experiments were performed using 100 mg L^{-1} of initial dye concentration and NaCl concentration was varied from 0.01 to 0.1 mol L^{-1}. The obtained results have been depicted in Fig. 5. It can be seen from the figure that biosorption capacity marginally decreased from 32.8 ± 0.18 to 29.11 ± 0.32 mg g^{-1} with an increase in salt concentration from 0.01 to 0.1 mol L^{-1}. It can be attributed to competition between dye anion and inorganic salt anion for adsorption on biosorbent [57]. Similar trend has been reported for removal of anionic dyes using carbon nanotubes [58]. It is also important to note that the extent of decrease was not significant confirming that the present results can be equally applied to commercial effluents where salts might be present (appropriate care can be taken to slightly increase the adsorbent loading).

3.7. Adsorption kinetics

3.7.1. Pseudo first-order model

The obtained values for the pseudo first-order model constants are depicted in Table 2. The correlation coefficient (R^2) values (average value 0.9766) are not very closer to unity and the $q_{e,exp}$ and $q_{e,cal}$ values are significantly deviating from each other as seen from Table 2, which suggests that the adsorption process did not follow pseudo first-order kinetics. However, adsorption process followed first-order kinetics for AB 113 dye removal using commercial activated carbon and rubber tire derived carbon [31] possibly indicating that the trend depends on the type of controlling mechanisms and hence the importance of current work of kinetic model fitting is established.

3.7.2. Pseudo second-order model

The obtained values for the pseudo second-order model constants are depicted in Table 2. It can be seen from Table 2 that the correlation coefficient, R^2 values (average value 0.9991) are very close to unity and $q_{e,exp}$ and $q_{e,cal}$ values are also very close to each other for all the studied concentrations. These findings suggested better fitting of pseudo second-order kinetics to the current adsorption system. Similar results have been reported for the removal of AB 113 using activated red mud [6] and AB 25 using NaOH treated ficus racemosa [26]. Increase in initial dye concentration from 50 to 200 mg L^{-1}, led to a decrease in pseudo second-order rate constant values (k_2) from 0.0074 to 0.0008 g mg^{-1} min^{-1}, respectively confirming that extent of biosorption of AB 113 on SMPD is inversely dependent on initial dye concentration. Similar trend has also been reported for removal of Astrazon Yellow 7GL from aqueous solutions using wheat bran [59].

Table 2
Kinetic parameters for removal of AB 113 by SMPD (T = 303 K, t = 5 h, m = 3 g L^{-1}).

Pseudo first-order model

C_i (mg L^{-1})	$q_{e,exp}$ (mg g^{-1})	$q_{e,cal}$ (mg g^{-1})	k_1 (min^{-1})	R^2
50	16.61	12.28	0.0388	0.9889
100	33.03	48.61	0.0387	0.9641
150	48.47	55.84	0.0303	0.9753
200	60.97	67.65	0.0280	0.9779

Pseudo second- order model

C_i (mg L^{-1})	$q_{e,exp}$ (mg g^{-1})	$q_{e,cal}$ (mg g^{-1})	k_2 (g mg^{-1} min^{-1})	R^2
50	16.61	17.24	0.0074	0.9992
100	33.03	34.84	0.0023	0.9993
150	48.47	52.08	0.0011	0.9990
200	60.97	66.23	0.0008	0.9989

Weber- Morris intra-particle diffusion model

C_i (mg L^{-1})	k_{id} (mg g^{-1} $min^{-1/2}$)	C (mg g^{-1})	Section	R^2
50	1.156	6.00	First	0.9882
100	2.403	9.88	First	0.9905
150	3.687	10.72	First	0.9913
200	4.688	11.61	First	0.9856
50	0.027	16.20	Second	0.6227
100	1.016	20.98	Second	0.9948
150	1.398	30.87	Second	0.9701
200	1.453	41.75	Second	0.9746
100	0.067	31.87	Third	0.5899
150	0.096	46.90	Third	0.7862
200	0.117	59.02	Third	0.8014

Bangham pore diffusion model

C_i (mg L^{-1})	α	k_0	R^2
50	0.678	2.61	0.9414
100	0.660	2.23	0.9734
150	0.615	2.15	0.9748
200	0.534	2.42	0.9631

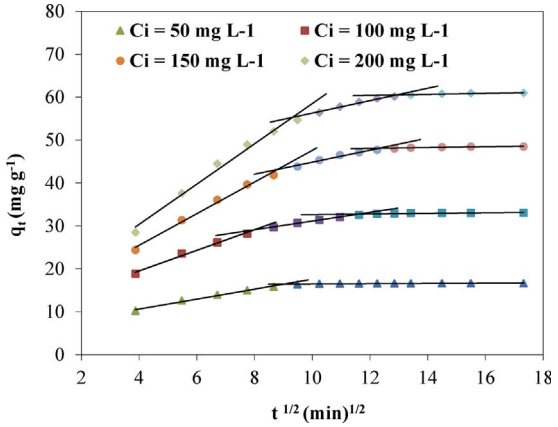

Fig. 6. Weber-Morris intra-particle diffusion plot for removal of AB 113 by SMPD (T = 303 K, t = 5 h, C_i = 50–200 mg L^{-1}, m = 3 g L^{-1}).

3.7.3. Intra-particle diffusion model

The obtained plot of q_t against $t^{1/2}$ for all the studied dye concentrations is depicted in Fig. 6. If the plot passes through the origin then intra-particle diffusion is the only rate controlling step [60]. As seen from Fig. 6, none of the lines for all the studied concentrations passed through the origin, indicating that intra-particle diffusion was not the sole rate controlling step. Multi-linearity with different slopes is observed for all the studied dye concentrations, indicating presence of

more than one kinetic mechanism governing the biosorption of AB 113 [61]. The first sharper section with higher slope is the external surface biosorption driven where rapid diffusion of dye occurs to the external surface of the biosorbent. The second section represents the gradual biosorption stage, where intra-particle diffusion is rate controlling step. The third section represents final stage of equilibrium indicating saturation of the biosorbent surface where the diffusion starts to slow down due to either the extremely low concentration of dye remaining in the solution or attainment of maximum dye adsorption possible at equilibrium [14,52]. Referring to Fig. 6, it can be said that two stage behavior was observed for 50 mg L^{-1} of dye concentration and distinct three stage behavior was observed for higher dye concentrations of 100, 150 and 200 mg L^{-1}. The values of k_{id} and C obtained from the plot are summarized in Table 2. Value of C indicates boundary layer thickness. Larger value of C indicates greater boundary layer effect [62]. It was observed that with an increase in initial AB 113 dye concentration from 50 to 200 mg L^{-1}, the values of C increased (Table 2) for all stages indicating increase in boundary layer thickness.

3.7.4. Bangham pore diffusion model

Kinetic data in present study was also analyzed by Bangham model. Bangham model is used to check whether pore diffusion is the sole rate controlling step. The obtained model parameter values have been given in Table 2. If double logarithmic plot of Eq. (7) yields a perfect linear curve then pore diffusion is the only rate limiting step. In present study, the perfect fitting of linear curves (correlation coefficient close to 1) for all studied concentrations was not observed indicating that diffusion of dye into the pores of biosorbent was involved in biosorption process but it was not the sole rate limiting step. It was observed that both steps of film and pore diffusion were important and contributing to some extents in deciding the final extent of adsorption obtained in the present study. The obtained findings confirmed that there are different steps involved in the adsorption of AB 113 dye on SMPD biosorbent. Similar trend has been also reported for removal of congo red dye using ferrocene based mesoporous material [63].

3.8. Effect of temperature

Biosorption capacity is significantly affected by temperature. Change in temperature affects the equilibrium biosorption capacity of the adsorbent for a particular dye. Biosorption experiments were conducted at different temperatures and adsorption equilibrium curve was plotted to investigate the dependency. Fig. 7 depicts the plot of biosorption capacity of SMPD at equilibrium (q_e) against equilibrium dye concentration, C_e at four different temperatures of 293, 303, 313 and 323 K. The biosorption capacity decreased with an increase in the temperature indicating that adsorption is exothermic in nature [64]. The maximum biosorption capacity, q_m decreased from 97.09 to 86.96 mg g^{-1} with an increase in temperature from 293 to 323 K. Increase in temperature decreased biosorption capacity due to weakening of the physical bonds between the AB 113 dye molecules and the active sites of the biosorbent at higher temperatures. Decrease in biosorption capacity with an increase in temperature may also be due to tendency of AB 113 dye molecules to escape from biosorbent surface to bulk phase due to an possible increase in solubility. Similar trend and exothermic nature has been reported for the removal of AB 113 by activated carbon prepared from waste rubber tire [31] and Malachite Green using adsorbent based on sea shell powder [43].

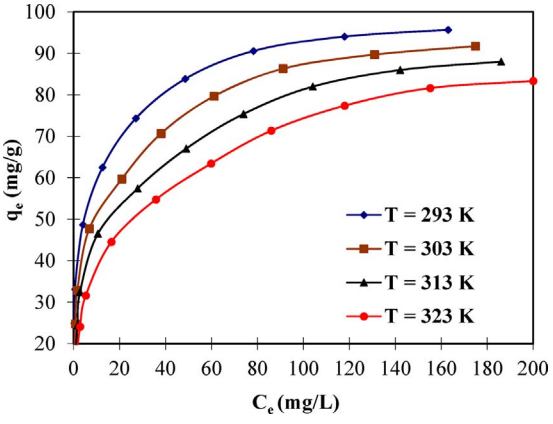

Fig. 7. Equilibrium adsorption isotherms for removal of AB 113 by SMPD at different temperatures (t = 2.5 h, C_i = 50–450 mg L^{-1}, m = 3 g L^{-1}).

Table 3
Isotherm parameters for removal of AB 113 by SMPD (t = 2.5 h, C_i = 50–450 mg L^{-1}, m = 3g L^{-1}).

Freundlich model: $q_e = K_F C_e^{1/n}$

T (K)	K_F (mg g^{-1})/(mg L^{-1}) $^{1/n}$	$1/n$	R^2	ARE
293	32.93	0.232	0.9816	6.73
303	26.42	0.261	0.9838	5.87
313	21.52	0.287	0.9829	5.68
323	17.50	0.311	0.9897	4.31

Langmuir model: $q_e = \frac{q_m K_L C_e}{1 + K_L C_e}$

T (K)	K_L (L mg^{-1})	q_m (mg g^{-1})	R^2	ARE
293	0.253	97.09	0.9975	26.01
303	0.157	93.46	0.9956	22.32
313	0.108	90.09	0.9937	19.03
323	0.076	86.96	0.9925	16.48

Temkin model: $q_e = B_1 \ln (K_T C_e)$

T (K)	K_T (L mg^{-1})	B_1 (mg g^{-1})	R^2	ARE
293	30.67	11.23	0.9893	5.79
303	9.88	12.21	0.9887	5.45
313	4.25	13.01	0.9890	5.55
323	2.19	13.48	0.9863	6.16

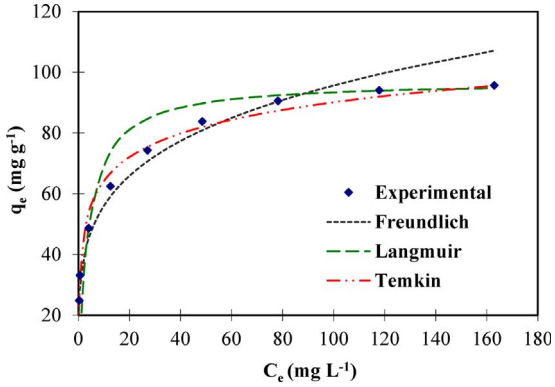

Fig. 8. Comparison of $q_{e,exp}$ with $q_{e,cal}$ obtained from various isotherm models for removal of AB 113 by SMPD (t = 2.5 h, C_i = 50–450 mg L^{-1}, m = 3 g L^{-1}).

3.9. Biosorption equilibrium study

The capacity of the adsorbent is typically determined using equilibrium study. Isotherm data were subjected to fitting using different models and the obtained results of linear regression were used to determine the best fit among different models used. Obtained values of isotherm parameters and correlation coefficient (R^2) have been given in Table 3. Among all the models studied, correlation coefficient, R^2 values were very close to unity for Langmuir model (average value 0.9948) and Temkin model (average value 0.9883) indicating better

Table 4
Activation energy and thermodynamic parameters for biosorption of AB 113 onto SMPD.

E_a (kJ mol^{-1})	ΔG^0 (kJ mol^{-1})				ΔH^0 (kJ mol^{-1})	ΔS^0 (kJ mol^{-1} K^{-1})
	293 K	303 K	313 K	323 K		
6.54	−29.383	−29.194	−29.181	−29.167	−31.34	−0.007

Table 5
Maximum adsorption capacity (q_m) for removal of various acidic dyes from aqueous solution using different adsorbents based on literature.

Anionic and azo dyes	Adsorbents	q_m (mg g^{-1})	pH	Temperature T (K)	Adsorbent dose (g L^{-1})	Reference
AB 113	SMPD	**97.09**	6.5	293	3	Present study
AB 113	NTPD	**25.51**	6.5	293	10	Present study
AB 113	Overripe Cucumis sativus peel	59.81	2	323	8	[69]
AB 113	Activated red mud	83.33	3	298	6	[6]
AB 113	Commercial activated carbon	7.84	5	298	5	[31]
AB 113	Rubber tire activated carbon	9.72	2	298	10	[31]
AB 25	Alkali treated sawdust	24.39	2	300	2	[70]
Acid orange 7	Natural pumice	15.56	7	298	3.2	[71]
Acid orange 7	Fe-coated pumice	27.68	9	298	3.2	[71]
Acid orange 10	Activated sugarcane bagasse	5.78	2.3	313	2	[72]
Acid red 18	Surfactant modified zeolite	20.42	3	298	4	[73]
Congo red	Surfactant modified tea waste	106.4	–	303	4	[33]
Congo red	Ceram kaolin	8.97	3	298	5	[62]
Congo red	Surfactant modified pumice	27.32	8	298	10	[74]

fitting of these models to the obtained experimental results. The data given in Table 3 also confirm a decrease in q_m and K_L for the Langmuir model and K_T for the Temkin model with an increase in temperature confirming the exothermic nature of the adsorption process.

ARE values obtained have been given in Table 3. It can be seen from Table 3 that ARE error values are found to be minimum for the Temkin model as compared to other isotherms. Fig. 8 represents the parity plot of $q_{e,exp}$ values with $q_{e,cal}$ values for the various isotherm models studied (variation with C_e has been represented). Referring to Fig. 8, it can be said that at lower concentration range, $q_{e,cal}$ values using Temkin model are closer to the $q_{e,exp}$ values and at higher concentration range, $q_{e,cal}$ values using Langmuir model are closer to the $q_{e,exp}$ values. The correlation coefficient, R^2 values were found to be the best for the Langmuir isotherm with marginally lower values for Temkin model. Overall, it can be said that equilibrium data of adsorption in present study was equally best fitted to Langmuir and Temkin isotherms.

3.10. Adsorption thermodynamics

Thermodynamic parameters have been evaluated from the graph of $ln\ K$ versus $1/T$ and shown in Table 4. At all temperatures studied, values of ΔG^0 have been found to be negative which confirms feasibility and spontaneous nature of the biosorption of AB 113 on SMPD biosorbent. Values of ΔH^0 have been found to be negative indicating exothermic nature of the biosorption [65]. The result was also confirmed from the earlier results of decrease in q_e values with an increase in temperature [66]. Similar trend has also been reported for the removal of Reactive Red 120 by clay [67]. Negative value of ΔS^0 indicated decreased randomness at the solid/solution interface during adsorption of dye on SMPD [68]. Similar trend has also been reported for the removal of congo red using kaolin and zeolite [14].

The obtained result for activation energy has also been depicted in Table 4. The type of biosorption, either physical or chemical can be predicted from the magnitude of activation energy. Physical biosorption is characterized by low activation energies (5–50 kJ mol^{-1}) whereas chemical biosorption is characterized by high activation energies (60–800 kJ mol^{-1}) [22]. In the present study, the activation energy for biosorption was found as 6.54 kJ mol^{-1}, confirming that biosorption of AB 113 on SMPD is physical in nature.

3.11. Comparison with other adsorbents

To establish the potential of SMPD as biosorbent for AB 113 dye removal from aqueous solution and in general for other effluents, the obtained maximum biosorption capacities in the present study have been compared with some of the adsorbents whose q_m values have been reported in the literature for different acidic dyes removal (Table 5). It can be established from Table 5 that synthesized SMPD biosorbent has comparatively higher q_m value as 97.09 mg g^{-1}. Hence SMPD biosorbent synthesized in the present study has been found to have better potential. Overall, it can be said that in comparison to other biosorbents, the main advantage is the higher adsorption capacity which is attributed to the activation treatment using surfactant. The synthesis of an effective biosorbent from the abundantly available waste biomass would be of much higher commercial interest and hence the findings of the present work are very important.

3.12. Reusability study

Potential of the adsorbent is decided by its reusability. Hence it is necessary to recover the spent adsorbent after dye removal. In the

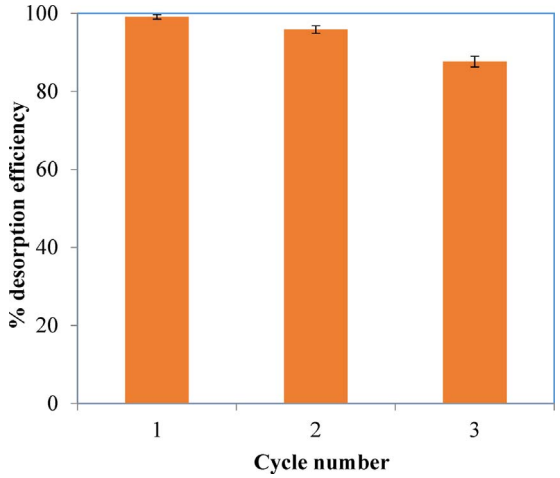

Fig. 9. Results of desorption efficiency for Regeneration and reuse of biosorbent.

present study, spent biosorbent is regenerated by a green solvent, ethanol. Regeneration results obtained for three adsorption-desorption cycles are depicted in Fig. 9. It was observed that desorption efficiency drops from 99.02 ± 0.57 for first cycle to 86.89 ± 1.38% for third cycle. These marginal losses can be due to the fact that small quantum of activity of biosorbent can be lost during adsorption- desorption cycle including the regeneration protocol. The obtained results indicated that spent adsorbent in the present study can be regenerated and reused efficiently with some degree of makeup loading that would be required to yield constant removal of effluents.

4. Conclusions

In the present study, dye removal was performed using biosorbent obtained from fallen leaves of *Prunus Dulcis*, a waste biomass which is available in abundance at much lower cost as compared to more commonly used commercial activated carbon. The NaOH and surfactant used for activation increased the cost of the synthesis process but the biosorption capacity and hence dye removal is significantly increased due to NaOH and surfactant activation and hence the enhanced costs of synthesis are offset. The regeneration of the adsorbent could be carried out using ethanol as a green solvent, whereas activated carbon suffers from problem of regeneration difficulty. These factors indicated environmental sustainability of the overall approach presented in the current work. The actual textile dye effluent contains salt and hence in present study, effect of salt on dye removal has also been investigated and it was established that presence of salt only marginally affected the dye removal. The obtained results in the present work clearly demonstrated that the dye removal was found to be almost 100% for 100 mg L^{-1} of initial dye concentration in a contact time of 2.5 h at 293 K. Maximum dye removal with minimum biosorbent dose was obtained by SMPD as compared to NTPD. Kinetic study also confirmed that biosorption follows three different phases of adsorption especially at higher initial dye concentrations. The maximum biosorption capacity was obtained as 97.09 mg g^{-1} by SMPD at temperature of 293 K, which was higher than the more commonly reported values. Overall, it can be said that the SMPD fallen leaves, a waste biomass can be successfully converted into effective and low cost biosorbent to remove AB 113, azo dye from aqueous solution such that the harmful effects associated with the contamination of dye in water can be eliminated.

Acknowledgements

The authors gratefully acknowledge University Grant Commission (UGC) for assistance under the UGC-Networking Resource Centre (NRC), at the Institute of Chemical Technology, Matunga.

References

[1] N. Thinakaran, P. Panneerselvam, P. Baskaralingam, D. Elango, S. Sivanesan, Equilibrium and kinetic studies on the removal of Acid Red 114 from aqueous solutions using activated carbons prepared from seed shells, J. Hazard. Mater. 158 (2008) 142–150.
[2] M.H. Farzana, S. Meenakshi, Decolorization and detoxification of Acid blue 158 dye using cuttlefish bone powder as co-adsorbent via photocatalytic method, J. Water Process Eng. 2 (2014) 22–30.
[3] E. Akceylan, M. Bahadir, M. Yılmaz, Removal efficiency of a calix [4] arene-based polymer for water-soluble carcinogenic direct azo dyes and aromatic amines, J. Hazard. Mater. 162 (2009) 960–966.
[4] M. Solís, A. Solís, H.I. Pérez, N. Manjarrez, M. Flores, Microbial decolouration of azo dyes: a review, Process Biochem. 47 (2012) 1723–1748.
[5] R.L. Singh, P.K. Singh, R.P. Singh, Enzymatic decolorization and degradation of azo dyes − a review, Int. Biodeterior. Biodegrad. 104 (2015) 21–31.
[6] M. Shirzad-Siboni, S.J. Jafari, O. Giahi, I. Kim, S. Lee, J. Yang, Removal of acid blue 113 and reactive black 5 dye from aqueous solutions by activated red mud, J. Ind. Eng. Chem. 20 (2014) 1432–1437.
[7] M.T. Yagub, T.K. Sen, S. Afroze, H.M. Ang, Dye and its removal from aqueous solution by adsorption: a review, Adv. Colloid Interface Sci. 209 (2014) 172–184.
[8] M. Toor, B. Jin, S. Dai, V. Vimonses, Activating natural bentonite as a cost-effective adsorbent for removal of Congo-red in wastewater, J. Ind. Eng. Chem. 21 (2015) 653–661.
[9] M. Koch, A. Yediler, D. Lienert, G. Insel, A. Kettrup, Ozonation of hydrolyzed azo dye reactive yellow 84 (CI), Chemosphere 46 (2002) 109–113.
[10] M.K. Purkait, S.S. Vijay, S. DasGupta, S. De, Separation of Congo Red by surfactant mediated cloud point extraction, Dye Pigm. 63 (2004) 151–159.
[11] S. Mozia, M. Tomaszewska, A.W. Morawski, Photocatalytic degradation of azo-dye acid red 18, Desalination 185 (2005) 449–456.
[12] D.C. de Moura, M.A. Quiroz, D.R. da Silva, R. Salazar, C.A. Martínez-Huitle, Electrochemical degradation of acid blue 113 dye using TiO_2-nanotubes decorated with PbO2 as anode, environ nanotechnology, Monit. Manage. 5 (2016) 13–20.
[13] N.H.H. Hairom, A.W. Mohammad, A.A.H. Kadhum, Nanofiltration of hazardous Congo red dye: performance and flux decline analysis, J. Water Process Eng. 4 (2014) 99–106.
[14] V. Vimonses, S. Lei, B. Jin, C.W.K. Chow, C. Saint, Kinetic study and equilibrium isotherm analysis of Congo Red adsorption by clay materials, Chem. Eng. J. 148 (2009) 354–364.
[15] X. Yuan, X. Shi, S. Zeng, Y. Wei, Activated carbons prepared from biogas residue: characterization and methylene blue adsorption capacity, J. Chem. Technol. Biotechnol. 86 (2011) 361–366.
[16] L. Sun, S. Wan, W. Luo, Biochars prepared from anaerobic digestion residue, palm bark, and eucalyptus for adsorption of cationic methylene blue dye: characterization equilibrium, and kinetic studies, Bioresour. Technol. 140 (2013) 406–413.
[17] Y. Kismir, A.Z. Aroguz, Adsorption characteristics of the hazardous dye Brilliant Green on Saklıkent mud, Chem. Eng. J. 172 (2011) 199–206.
[18] S. Sadaf, H.N. Bhatti, S. Nausheen, M. Amin, Application of a novel lignocellulosic biomaterial for the removal of Direct Yellow 50 dye from aqueous solution: batch and column study, J. Taiwan Inst. Chem. Eng. 47 (2015) 160–170.
[19] K.Z. Elwakeel, A.M. Elgarahy, S.H. Mohammad, Use of beach bivalve shells located at Port Said coast (Egypt) as a green approach for methylene blue removal, J. Environ. Chem. Eng. 5 (2017) 578–587.
[20] D. Pathania, A. Sharma, Z. Siddiqi, Removal of congo red dye from aqueous system using Phoenix dactylifera seeds, J. Mol. Liq. 219 (2016) 359–367.
[21] S. Khamparia, D. Jaspal, Investigation of adsorption of Rhodamine B onto a natural adsorbent Argemone mexicana, J. Environ. Manage. 183 (2016) 786–793.
[22] F. Deniz, S.D. Saygideger, Equilibrium, kinetic and thermodynamic studies of Acid Orange 52 dye biosorption by Paulownia tomentosa Steud. leaf powder as a low-cost natural biosorbent, Bioresour. Technol. 101 (2010) 5137–5143.
[23] M.M. Hamed, I.M. Ahmed, S.S. Metwally, Adsorptive removal of methylene blue as organic pollutant by marble dust as eco-friendly sorbent, J. Ind. Eng. Chem. 20 (2014) 2370–2377.
[24] V.M. Vucurovic, R.N. Razmovski, M.N. Tekic, Methylene blue (cationic dye) adsorption onto sugar beet pulp: equilibrium isotherm and kinetic studies, J. Taiwan Inst. Chem. Eng. 43 (2012) 108–111.
[25] M.A.M. Salleh, D.K. Mahmoud, W.A.W.A. Karim, A. Idris, Cationic and anionic dye adsorption by agricultural solid wastes: a comprehensive review, Desalination 280 (2011) 1–13.
[26] S.N. Jain, P.R. Gogate, NaOH-treated dead leaves of Ficus racemosa as an efficient biosorbent for Acid Blue 25 removal, Int. J. Environ. Sci. Technol. 14 (2017) 531–542.
[27] V.K. Garg, M. Amita, R. Kumar, R. Gupta, Basic dye (methylene blue) removal from simulated wastewater by adsorption using Indian Rosewood sawdust: a timber industry waste, Dye Pigm. 63 (2004) 243–250.
[28] G.K. Sarma, S. Sen Gupta, K.G. Bhattacharyya, Adsorption of Crystal violet on raw and acid-treated montmorillonite K10, in aqueous suspension, J. Environ. Manage. 171 (2016) 1–10.
[29] B. Zhao, Y. Shang, W. Xiao, C. Dou, R. Han, Adsorption of Congo red from solution using cationic surfactant modified wheat straw in column model, J. Environ. Chem. Eng. 2 (2014) 40–45.
[30] L. Lian, L. Guo, A. Wang, Use of CaCl2 modified bentonite for removal of Congo red dye from aqueous solutions, Desalination 249 (2009) 797–801.
[31] V.K. Gupta, B. Gupta, A. Rastogi, S. Agarwal, A. Nayak, A comparative investigation on adsorption performances of mesoporous activated carbon prepared from waste rubber tire and activated carbon for a hazardous azo dye — Acid Blue 113, J. Hazard. Mater. 186 (2011) 891–901.
[32] L. Wang, A. Wang, Adsorption properties of Congo Red from aqueous solution onto surfactant-modified montmorillonite, J. Hazard. Mater. 160 (2008) 173–180.
[33] M. Foroughi-dahr, H. Abolghasemi, M. Esmaieli, G. Nazari, B. Rasem, Experimental study on the adsorptive behavior of Congo red in cationic surfactant-modified tea waste, Process Saf. Environ. Prot. 95 (2015) 226–236.
[34] N. Mohan, N. Balasubramanian, V. Subramanian, Electrochemical treatment of simulated textile effluent, Chem. Eng. Technol. 24 (2001) 749–753.
[35] S. Lagergren, About the theory of so called adsorption of soluble substances, Ksver Veterskapsakad Handl. 24 (1898) 1–6.
[36] Y.S. Ho, G. Mckay, Pseudo-second order model for sorption processes, Process Biochem. 34 (1999) 451–465.
[37] W.J. Weber, J. Carrell Morris, Kinetics of adsorption on carbon from solution, J. Sanit. Eng. Div. Am. Soc. Civ. Eng. 89 (1963) 31–60.
[38] D.H. Bangham, F.P. Burt, The behaviour of gases in contact with glass surfaces, Proc. R. Soc. Lond. Ser. A Contain Pap. Math Phys. Charact. 105 (1924) 481–488.
[39] H.M.F. Freundlich, Over the adsorption in solution, J. Phys. Chem. 57 (1906) 385–470.
[40] I. Langmuir, The adsorption of gases on plane surfaces of glass, mica and platinum, J. Am. Chem. Soc. 40 (1918) 1361–1403.
[41] M.J. Temkin, V. Pyzhev, Recent modifications to Langmuir isotherms, Acta Physicochim. USSR 12 (1940) 217–225.
[42] A. Kapoor, R.T. Yang, Correlation of equilibrium adsorption data of condensible vapours on porous adsorbents, Gas Sep. Purif. 3 (1989) 187–192.

[43] S. Chowdhury, P. Saha, Sea shell powder as a new adsorbent to remove Basic Green 4 (Malachite Green) from aqueous solutions: equilibrium, kinetic and thermodynamic studies, Chem. Eng. J. 164 (2010) 168–177.
[44] A.B. Albadarin, M.N. Collins, M. Naushad, S. Shirazian, G. Walker, C. Mangwand, Activated lignin-chitosan extruded blends for efficient adsorption of methylene blue, Chem. Eng. J. 307 (2017) 264–272.
[45] A.A. El-zahhar, N.S. Awwad, Removal of malachite green dye from aqueous solutions using organically modified hydroxyapatite, J. Environ. Chem. Eng. 4 (2016) 633–638.
[46] Y. Yang, D. Jin, G. Wang, S. Wang, X. Jia, Y. Zhao, Competitive biosorption of acid blue 25 and acid red 337 onto unmodified and CDAB-modified biomass of aspergillus oryzae, Bioresour. Technol. 102 (2011) 7429–7436.
[47] V.S. Munagapati, D. Kim, Adsorption of anionic azo dye Congo red from aqueous solution by cationic modified orange peel powder, J. Mol. Liq. 220 (2016) 540–548.
[48] G.G. Sonai, M.A. Selene, G.U. de Souza, D. de Oliveira, A.A.U. de Souza, The application of textile sludge adsorbents for the removal of Reactive Red 2 dye, J. Environ. Manage. 168 (2016) 149–156.
[49] R. Lafi, A. Hafiane, Removal of methyl orange (MO) from aqueous solution using cationic surfactants modified coffee waste (MCWs), J. Taiwan Inst. Chem. Eng. 58 (2016) 424–433.
[50] Z. Yan, J. Li, S. Chang, T. Cui, Y. Jiang, M. Yu, L. Zhang, G. Zhao, P. Qi, S. Li, Lignin relocation contributed to the alkaline pretreatment efficiency of sweet sorghum bagasse, Fuel 158 (2015) 152–158.
[51] C. Xia, Y. Jing, Y. Jia, D. Yue, J. Ma, X. Yin, Adsorption properties of congo red from aqueous solution on modified hectorite: kinetic and thermodynamic studies, Desalination 265 (2011) 81–87.
[52] S. Chen, J. Zhang, C. Zhang, Q. Yue, Y. Li, C. Li, Equilibrium and kinetic studies of methyl orange and methyl violet adsorption on activated carbon derived from Phragmites australis, Desalination 252 (2010) 149–156.
[53] V. da S. Lacerda, J.B. López-Sotelo, A. Correa-Guimarães, S. Hernández-Navarro, M. Sánchez-Báscones, L.M. Navas-Gracia, P. Martín-Ramos, J. Martín-Gil, Rhodamine B removal with activated carbons obtained from lignocellulosic waste, J. Environ. Manage. 155 (2015) 67–76.
[54] Q. Du, J. Sun, Y. Li, X. Yang, X. Wang, Z. Wang, L. Xia, Highly enhanced adsorption of congo red onto graphene oxide/chitosan fibers by wet-chemical etching off silica nanoparticles, Chem. Eng. J. 245 (2014) 99–106.
[55] V.S. Mane, P.V.V. Babu, Studies on the adsorption of Brilliant Green dye from aqueous solution onto low-cost NaOH treated saw dust, Desalination 273 (2011) 321–329.
[56] M. Laabd, H.A. Ahsaine, A. El Jaouhari, B. Bakiz, M. Bazzaoui, M. Ezahri, A. Albourine, A. Benlhachem, Congo red removal by PANi/Bi_2WO_6 nanocomposites: kinetic, equilibrium and thermodynamic studies, J. Environ. Chem. Eng. 4 (2016) 3096–3105.
[57] J. Wang, H. Zhu, C. Hurren, J. Zhao, E. Pakdel, Z. Li, X. Wang, Degradation of organic dyes by P25-reduced graphene oxide: influence of inorganic salts and surfactants, J. Environ. Chem. Eng. 3 (2015) 1437–1443.
[58] A. Maleki, U. Hamesadeghi, H. Daraei, B. Hayati, F. Najafi, G. Mckay, R. Rezaee, Amine functionalized multi-walled carbon nanotubes: single and binary systems for high capacity dye removal, Chem. Eng. J. 313 (2016) 826–835.
[59] M.T. Sulak, E. Demirbas, M. Kobya, Removal of Astrazon Yellow 7GL from aqueous solutions by adsorption onto wheat bran, Bioresour. Technol. 98 (2007) 2590–2598.
[60] M.A. Ahmad, N.K. Rahman, Equilibrium, kinetics and thermodynamic of Remazol Brilliant Orange 3R dye adsorption on coffee husk-based activated carbon, Chem. Eng. J. 170 (2011) 154–161.
[61] M. Ugurlu, Adsorption of a textile dye onto activated sepiolite, Microporous Mesoporous Mater. 119 (2009) 276–283.
[62] V. Vimonses, S. Lei, B. Jin, C.W.K. Chow, C. Saint, Adsorption of congo red by three Australian kaolins, Appl. Clay Sci. 43 (2009) 465–472.
[63] S. Kaur, S. Rani, V. Kumar, R.K. Mahajan, M. Asif, I. Tyagi, V.K. Gupta, Synthesis, characterization and adsorptive application of ferrocene based mesoporous material for hazardous dye Congo red, J. Ind. Eng. Chem. 26 (2014) 234–242.
[64] M. Dogan, M.H. Karaoglu, M. Alkan, Adsorption kinetics of maxilon yellow 4GL and maxilon red GRL dyes on kaolinite, J. Hazard. Mater. 165 (2009) 1142–1151.
[65] F. Deniz, S.D. Saygideger, Removal of a hazardous azo dye (Basic Red 46) from aqueous solution by princess tree leaf, Desalination 268 (2011) 6–11.
[66] Y. Chen, D. Zhang, Adsorption kinetics, isotherm and thermodynamics studies of flavones from Vaccinium Bracteatum Thunb leaves on NKA-2 resin, Chem. Eng. J. 254 (2014) 579–585.
[67] E. Errais, J. Duplay, F. Darragi, I. M'Rabet, A. Aubert, F. Huber, G. Morvan, Efficient anionic dye adsorption on natural untreated clay: kinetic study and thermodynamic parameters, Desalination 275 (2011) 74–81.
[68] M.A. Ahmad, R. Alrozi, Removal of malachite green dye from aqueous solution using rambutan peel-based activated carbon: equilibrium, kinetic and thermodynamic studies, Chem. Eng. J. 171 (2011) 510–516.
[69] L.Y. Lee, S. Gan, M.S.Y. Tan, S.S. Lim, X.J. Lee, Y.F. Lam, Effective removal of Acid Blue 113 dye using overripe Cucumis sativus peel as an eco-friendly biosorbent from agricultural residue, J. Clean. Prod. 113 (2016) 194–203.
[70] M.A.K.M. Hanafia, W.S.W. Ngah, S.H. Zolkafly, L.C. Teong, Z.A.A. Majid, Acid Blue 25 adsorption on base treated Shorea dasyphylla sawdust: kinetic, isotherm, thermodynamic and spectroscopic analysis, J. Environ. Sci. 24 (2012) 261–268.
[71] B. Heibati, S. Rodriguez-Couto, N.G. Turan, O. Ozgonenel, A.B. Albadarin, M. Asif, I. Tyagi, S. Agarwal, V.K. Gupta, Removal of noxious dye—acid orange 7 from aqueous solution using natural pumice and Fe-coated pumice stone, J. Ind. Eng. Chem. 31 (2015) 124–131.
[72] W.T. Tsai, C.Y. Chang, M.C. Lin, S.F. Chien, H.F. Sun, M.F. Hsieh, Adsorption of acid dye onto activated carbons prepared from agricultural waste bagasse by $ZnCl_2$ activation, Chemosphere 45 (2001) 51–58.
[73] N. Mirzaei, M. Hadi, M. Gholami, R.F. Fard, M.S. Aminabad, Sorption of acid dye by surfactant modificated natural zeolites, J. Taiwan Inst. Chem. Eng. 59 (2016) 186–194.
[74] H. Shayesteh, A. Rahbar-Kelishami, R. Norouzbeigi, Evaluation of natural and cationic surfactant modified pumice for congo red removal in batch mode: kinetic, equilibrium, and thermodynamic studies, J. Mol. Liq. 221 (2016) 1–11.